A numerical method for the solid mechanics with Euler variables

A numerical method for the solid mechanics with Euler variables

Junchen Liu[1,*], Shihai Li[2], Ling Wang[1], Chun Feng[2], Feng Qian[1], Junfu Wang[1], Xinguang Zhu[2]

[1]School of Sciences, Changzhou Institute of Technology, China
[2]Institute of Mechanics, Chinese Academy of Sciences, Beijing, China

*E-mail: liujunchen22@126.com

Abstract. Based on the requirement of field engineering, we proposed a new numerical method for analyzing the solid mechanics with Euler variables. By replacing the Lagrange variables with the Euler variables, there will be three new items appearing in the equation. We use the fixed Euler grid to calculate solid mechanics, and use the boundary of material regiment to describe the movement of the boundary of material, after the boundary of material regiment moves beyond the Euler element grid size, new Euler element grids will appear and the corresponding old Euler element grids which have been out of the region of material will disappear. By this way, the movement of solid could be calculated in the Euler fixed grids. Then we did some test cases, we get the result that the new method is right and could be used to calculate the solid mechanic problems.

1. Introduction

Normally in the research, we compute the fluid mechanics with Euler variables, and the solid mechanics with Lagrange variables. While with the development of field engineering, new mechanical problems have been raised, such as, nowadays with more and more mining enterprises using interference radar monitoring technology to monitor the deformation of the slope of the open-pit mines, more and more researchers begin to focus on the problem how to use the interference radar monitoring data to analyze the stability of the slope (e.g., [1, 2, 3, 4, 5]). Due to the data gotten by the interference radar monitoring technology is based on the Eula coordinate system which means that this monitoring technology focus on monitoring the motion of the material at the fixed coordinate positions, while nowadays most numerical software used to analyze the solid mechanics is developed based on the Lagrange coordinate system, so a new mechanical problem has been improved, we need to develop the new numerical method for analyzing the solid mechanics based on the Euler coordinate system.

Actually for the numerical method analyzing solid mechanics in Euler coordinate system, there are many researchers studying on this problem all around the world, because they want to find a method to deal with the large deformation problem in solid mechanics, or they want to reduce the computation cost for the solid with very complex boundaries. With they researching on these problems, how to deal with the deformable boundaries of the solid model in Euler grids has been a topic of great interest for centuries (e.g.,[6-10]). Prof. Liu Chuanqi and his colleagues [11] have done a thorough research on this problem ,they proposed an implicit material point method designed to bypass meshing of bodies by employing level set functions to represent the boundaries at Euler grids. This implicit function representation provides an elegant mean to link an unbiased intermediate reference surface with the true boundaries by closest point projection as shown in Leichner et al. (2019). For this problem, other researchers also has done many studies, such as, in order to deal with the computational challenges of the multi-particle contact problems in assemblies of deformable bodies, a popular way is to simplify the nature of the contact by allowing overlapping of particles and then approximate the quasi-static responses with an explicit time integration scheme with an artificial damping [12-14]. Besides, an implicit function representation approach is often used to capture the interactions of particles of non-spherical shapes [15-16]. This scheme is firstly proposed in [15] by using level set, or signed distance function to identify the location of the particle boundaries. And then using a constrained optimization algorithm to compute the contacts and the overlapping distance of the particles. Additionally, there is an alternative but computationally more demanding approach, which is to explicitly model the deformation of particles and captures the evolution of contacts in a finite element (FE) framework. This algorithm has been extensively studied for decades. By designating master/slave (or mortar/non-mortar) pairs, contact constraints are imposed via node-to-segment [17-18], or segment-to-segment (latest mortar method) [19-21]. There are also many other researchers having done great achievements for this research, here we do not list them one by one because of the length of the article.

Compared with the above thorough researches on this question, we want to propose a new method to deal with our problem from a new view point. We compute the solid mechanics with Euler variables in the fixed Euler grids, and use the boundary of material regiment which is composed of the boundaries of the Euler element grids plus the displacement field within the elements to describe the movement of the boundary of material, after the boundary of material regiment moves beyond the Euler element grid size, new fixed Euler element grid will appear and the corresponding old Euler element grids which have been out of the region of solid materials will disappear. By this way, the movement and the deformation of the solid material could be calculated in the Euler fixed grids.

2. Discussion

Nowadays, normally we compute the solid mechanics under the Lagrange coordinate system which use the Lagrange grid, a kind of moving grid which moves with the solid, while we solve the fluid mechanics under the Euler coordinate system by using the Euler grid. The Euler grid is fixed grid and we focus on the motion of the material in the grid. In order to analyze the numerical method for analyzing the solid mechanics under Euler coordinate system, namely focusing on the solid mechanics in the fixed Euler grids, we need to understand the difference of the two kinds of methods under different coordinate system firstly. Here we need to know the two kinds of variables, Lagrange variables and Euler variables. Lagrange variable is the variable of time, while the Euler variable is variable of both spatial coordinates and time. So we need to use the Euler variables instead of the

Lagrange variables in the new method for analyzing the solid mechanics. Then there will be new items appearing in the equations. Secondly, we need to consider the problem that how to describe the movement of the Lagrange boundary of the solid in the fixed Euler grids. For this question, the concept of the material regiment was firstly raised by Prf. Li Shihai, namely we need to analyze the variation of the boundary of material regiment in the fixed Euler grids, which means that the description of the boundary of material regiment could be moved, while the Euler grid is fixed.

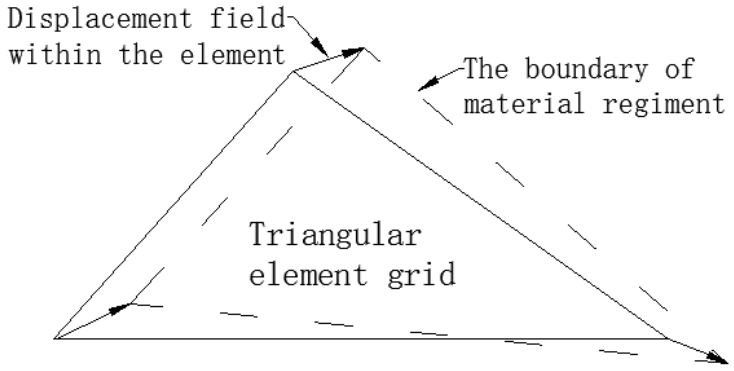

Fig. 1 The boundary of material regiment

Just as in Fig.1, The boundary of material regiment is composed of the boundary of the Euler element grid plus the displacement field within the element. By using the boundary of material regiment to describe the surface of the moving material, and calculating the variation of the boundary of material regiment, the dynamic boundary problem under Euler grid could be solved. Because the Euler grid is fixed grid, when the material moves, we use the boundary of material regiment to describe the movement of the boundary of material, and after the boundary of material regiment moves beyond the Euler element grid size, new Euler element grid will appear and the corresponding old Euler element grid will disappear. By this way, the movement of solid could be calculated in the Euler fixed grids.

By dealing with the momentum balance equation of the solid mechanics

$\nabla \cdot \sigma(\mathrm{u}) + F = \rho \frac{\partial^2 \mathrm{u}}{\partial t^2}$, in the weak formulation, the right hand side of the equation will become $\rho \int_\Omega \frac{\mathrm{d}v}{\mathrm{d}t} \mathrm{d}\Omega$. In order to analyze the numerical method for analyzing the solid mechanics under Euler coordinate system, we need to use the Euler variables to replace the Lagrange variables. Namely, in the new method, v is not only the variable of time, but also the variable of spatial coordinates. Then

$$\frac{D}{Dt}\int_{\Omega(t)} v(\mathrm{x},t)\mathrm{d}\Omega = \int_{\Omega(t)} \frac{\partial v(\mathrm{x},t)}{\partial t}\mathrm{d}\Omega + \int_{\Omega(t)} \nabla\cdot(v(\mathrm{x},t)\mathrm{v})\mathrm{d}\Omega$$
$$= \int_{\Omega_e} \frac{\partial v(\mathrm{x},t)}{\partial t}\mathrm{d}\Omega + \int_{\Omega_{LE}(t)} \frac{\partial v(\mathrm{x},t)}{\partial t}\mathrm{d}\Omega + \int_{\Omega_e} \nabla\cdot(v(\mathrm{x},t)\mathrm{v})\mathrm{d}\Omega + \int_{\Omega_{LE}(t)} \nabla\cdot(v(\mathrm{x},t)\mathrm{v})\mathrm{d}\Omega_{LE}$$

where $\Omega_{LE} = \Omega - \Omega_e$, Ω is the region of material regiment and Ωe is the region of fixed Euler grid elements.

According to the concept of divergence [26], just as in Fig. 2

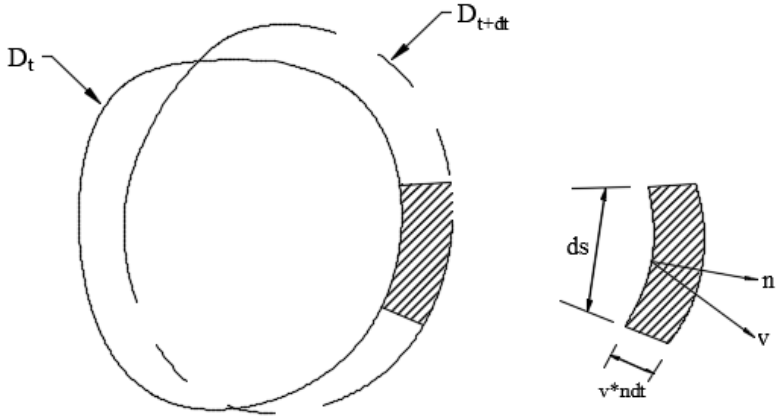

Fig. 2 Description of divergence

$$\mathrm{div}\, v = \nabla\cdot v = \lim_{\delta V\to 0}\frac{\int_S v\cdot \mathrm{n}\mathrm{d}S}{\delta V}$$

namely the velocity flux through the closed surface S, $\int_S v\cdot \mathrm{n}\mathrm{d}S$ equal to the rate of volume variation δV , so we have

$$\nabla\cdot v = \frac{1}{\delta V}\frac{\mathrm{d}}{\mathrm{d}t}\delta V$$

and

$$\int_{V(t)}\nabla\cdot(f(x,t)v)\delta V = \int_{\partial V(t)} f(x,t)v\cdot \mathrm{n}\delta S\ .$$

So

$$\int_{\Omega-\Omega_e} v(\nabla\cdot v)\mathrm{d}\Omega = \oint_{\partial(\Omega-\Omega_e)} v(v\cdot \mathrm{n})\mathrm{d}s$$

Then

$$\begin{aligned}
&\frac{D}{Dt}\int_{\Omega(t)} v(\mathrm{x},t)\mathrm{d}\Omega \\
&= \int_{\Omega_e} \frac{\partial v(\mathrm{x},t)}{\partial t}\mathrm{d}\Omega + \int_{\Omega_{LE}(t)} \frac{\partial v(\mathrm{x},t)}{\partial t}\mathrm{d}\Omega + \int_{\Omega_e} \nabla\cdot(v(\mathrm{x},t)\mathrm{v})\mathrm{d}\Omega + \int_{\partial\Omega_{LE}(t)} v(\mathrm{x},t)(\mathrm{v}\cdot\mathrm{n})\mathrm{d}\partial\Omega_{LE} \\
&= \int_{\Omega_e} \frac{\partial v(\mathrm{x},t)}{\partial t}\mathrm{d}\Omega + \int_{\Omega_{LE}(t)} \frac{\partial v(\mathrm{x},t)}{\partial t}\mathrm{d}\Omega + \int_{\Omega_e} (\mathrm{v}\cdot\nabla v(\mathrm{x},t) + v(\mathrm{x},t)\nabla\cdot\mathrm{v})\mathrm{d}\Omega + \int_{\partial\Omega_{LE}(t)} v(\mathrm{x},t)(\mathrm{v}\cdot\mathrm{n})\mathrm{d}\partial\Omega_{LE} \\
&= \int_{\Omega_e} \frac{\partial v(\mathrm{x},t)}{\partial t}\mathrm{d}\Omega + \int_{\Omega_{LE}(t)} \frac{\partial v(\mathrm{x},t)}{\partial t}\mathrm{d}\Omega + \int_{\Omega_e} \mathrm{v}\cdot\nabla v(\mathrm{x},t)\mathrm{d}\Omega + \int_{\Omega_e} v(\mathrm{x},t)\nabla\cdot\mathrm{v}\mathrm{d}\Omega + \int_{\partial\Omega_{LE}(t)} v(\mathrm{x},t)(\mathrm{v}\cdot\mathrm{n})\mathrm{d}\partial\Omega_{LE}
\end{aligned}$$

By introducing the test function

$$N_i = \frac{1}{2S}(a_i + b_i x + c_i y),$$

the displacement

$$u = \begin{Bmatrix} u_x \\ u_y \end{Bmatrix} = \begin{bmatrix} N_i & 0 & N_j & 0 & N_m & 0 \\ 0 & N_i & 0 & N_j & 0 & N_m \end{bmatrix} \begin{Bmatrix} u_{xi} \\ u_{yi} \\ u_{xj} \\ u_{yj} \\ u_{xm} \\ u_{ym} \end{Bmatrix}.$$

Then the item

$$\rho\int_{\Omega_e} \frac{\partial v}{\partial t}\mathrm{d}\Omega + \rho\int_{\Omega_{LE}} \frac{\partial v}{\partial t}\mathrm{d}\Omega = \frac{\rho S_\Omega}{12\Delta t} \begin{bmatrix} 2 & 0 & 1 & 0 & 1 & 0 \\ 0 & 2 & 0 & 1 & 0 & 1 \\ 1 & 0 & 2 & 0 & 1 & 0 \\ 0 & 1 & 0 & 2 & 0 & 1 \\ 1 & 0 & 1 & 0 & 2 & 0 \\ 0 & 1 & 0 & 1 & 0 & 2 \end{bmatrix} \left(\begin{bmatrix} v_{xi(n+1)} \\ v_{yi(n+1)} \\ v_{xj(n+1)} \\ v_{yj(n+1)} \\ v_{xm(n+1)} \\ v_{ym(n+1)} \end{bmatrix} - \begin{bmatrix} v_{xi(n)} \\ v_{yi(n)} \\ v_{xj(n)} \\ v_{yj(n)} \\ v_{xm(n)} \\ v_{ym(n)} \end{bmatrix} \right)$$

We let

$$V_2 = \int_{\Omega_e} \mathrm{v}\cdot\nabla v(\mathrm{x},t)\mathrm{d}\Omega + \int_{\Omega_e} v(\mathrm{x},t)\nabla\cdot\mathrm{v}\mathrm{d}\Omega + \int_{\partial\Omega_{LE}(t)} v(\mathrm{x},t)(\mathrm{v}\cdot\mathrm{n})\mathrm{d}\partial\Omega_{LE},$$

then

$$\frac{\rho}{\Delta t}\left(\begin{bmatrix} v_{xi(n+1)} \\ v_{yi(n+1)} \\ v_{xj(n+1)} \\ v_{yj(n+1)} \\ v_{xm(n+1)} \\ v_{ym(n+1)} \end{bmatrix} - \begin{bmatrix} v_{xi(n)} \\ v_{yi(n)} \\ v_{xj(n)} \\ v_{yj(n)} \\ v_{xm(n)} \\ v_{ym(n)} \end{bmatrix}\right) = \begin{bmatrix} 2 & 0 & 1 & 0 & 1 & 0 \\ 0 & 2 & 0 & 1 & 0 & 1 \\ 1 & 0 & 2 & 0 & 1 & 0 \\ 0 & 1 & 0 & 2 & 0 & 1 \\ 1 & 0 & 1 & 0 & 2 & 0 \\ 0 & 1 & 0 & 1 & 0 & 2 \end{bmatrix}^{-1} \frac{12}{S_L}(H - V_2)$$

where H is the joint forces.

So we only need to calculate the other three items, $\rho\int_{\Omega_e}(\mathrm{v}\cdot\nabla)v\mathrm{d}\Omega$, $\rho\int_{\Omega_e}v(\nabla\cdot\mathrm{v})\mathrm{d}\Omega$ and $\rho\oint_{\partial(\Omega-\Omega_e)}v(\mathrm{v}\cdot\mathrm{n})\mathrm{d}s$, and then push the item V2 into the joint forces, by this way, we could get the numerical results.

3. The first item

By introducing

$$a_i = x_j y_m - x_m y_j \quad a_j = x_m y_i - x_i y_m \quad a_m = x_i y_j - x_j y_i$$
$$b_i = y_j - y_m \quad , \quad b_j = y_m - y_i \quad , \quad b_m = y_i - y_j$$
$$c_i = x_m - x_j \quad c_j = x_i - x_m \quad c_m = x_j - x_i$$

The first item

$$\rho\int_{\Omega_e} v_j \frac{\partial v}{\partial x_j}\mathrm{d}\Omega = \frac{1}{24}\rho \begin{bmatrix} (2b_i v_{xi} + 2c_i v_{yi} + b_i v_{xj} + c_i v_{yj} + b_i v_{xm} + c_i v_{ym}) & 0 \\ 0 & (2b_i v_{xi} + 2c_i v_{yi} + b_i v_{xj} + c_i v_{yj} + b_i v_{xm} + c_i v_{ym}) \\ (b_i v_{xi} + c_i v_{yi} + 2b_i v_{xj} + 2c_i v_{yj} + b_i v_{xm} + c_i v_{ym}) & 0 \\ 0 & (b_i v_{xi} + c_i v_{yi} + 2b_i v_{xj} + 2c_i v_{yj} + b_i v_{xm} + c_i v_{ym}) \\ (b_i v_{xi} + c_i v_{yi} + b_i v_{xj} + c_i v_{yj} + 2b_i v_{xm} + 2c_i v_{ym}) & 0 \\ 0 & (b_i v_{xi} + c_i v_{yi} + b_i v_{xj} + c_i v_{yj} + 2b_i v_{xm} + 2c_i v_{ym}) \end{bmatrix}$$

$$\begin{bmatrix} (2b_j v_{xi} + 2c_j v_{yi} + b_j v_{xj} + c_j v_{yj} + b_j v_{xm} + c_j v_{ym}) & 0 \\ 0 & (2b_j v_{xi} + 2c_j v_{yi} + b_j v_{xj} + c_j v_{yj} + b_j v_{xm} + c_j v_{ym}) \\ (b_j v_{xi} + c_j v_{yi} + 2b_j v_{xj} + 2c_j v_{yj} + b_j v_{xm} + c_j v_{ym}) & 0 \\ 0 & (b_j v_{xi} + c_j v_{yi} + 2b_j v_{xj} + 2c_j v_{yj} + b_j v_{xm} + c_j v_{ym}) \\ (b_j v_{xi} + c_j v_{yi} + b_j v_{xj} + c_j v_{yj} + 2b_j v_{xm} + 2c_j v_{ym}) & 0 \\ 0 & (b_j v_{xi} + c_j v_{yi} + b_j v_{xj} + c_j v_{yj} + 2b_j v_{xm} + 2c_j v_{ym}) \end{bmatrix}$$

$$\begin{bmatrix} (2b_m v_{xi} + 2c_m v_{yi} + b_m v_{xj} + c_m v_{yj} + b_m v_{xm} + c_m v_{ym}) & 0 \\ 0 & (2b_m v_{xi} + 2c_m v_{yi} + b_m v_{xj} + c_m v_{yj} + b_m v_{xm} + c_m v_{ym}) \\ (b_m v_{xi} + c_m v_{yi} + 2b_m v_{xj} + 2c_m v_{yj} + b_m v_{xm} + c_m v_{ym}) & 0 \\ 0 & (b_m v_{xi} + c_m v_{yi} + 2b_m v_{xj} + 2c_m v_{yj} + b_m v_{xm} + c_m v_{ym}) \\ (b_m v_{xi} + c_m v_{yi} + b_m v_{xj} + c_m v_{yj} + 2b_m v_{xm} + 2c_m v_{ym}) & 0 \\ 0 & (b_m v_{xi} + c_m v_{yi} + b_m v_{xj} + c_m v_{yj} + 2b_m v_{xm} + 2c_m v_{ym}) \end{bmatrix} \begin{bmatrix} v_{xi}^{(n)} \\ v_{yi}^{(n)} \\ v_{xj}^{(n)} \\ v_{yj}^{(n)} \\ v_{xm}^{(n)} \\ v_{ym}^{(n)} \end{bmatrix}$$

4. The second item

The second item

$$\rho\int_{\Omega_e} v(\nabla\cdot v)\mathrm{d}\Omega = \frac{1}{24}\rho \begin{bmatrix} 2 & 0 & 1 & 0 & 1 & 0 \\ 0 & 2 & 0 & 1 & 0 & 1 \\ 1 & 0 & 2 & 0 & 1 & 0 \\ 0 & 1 & 0 & 2 & 0 & 1 \\ 1 & 0 & 1 & 0 & 2 & 0 \\ 0 & 1 & 0 & 1 & 0 & 2 \end{bmatrix} \begin{bmatrix} v_{xi}^{(n)} \\ v_{yi}^{(n)} \\ v_{xj}^{(n)} \\ v_{yj}^{(n)} \\ v_{xm}^{(n)} \\ v_{ym}^{(n)} \end{bmatrix} \left(\begin{bmatrix} b_i & c_i & b_j & c_j & b_m & c_m \end{bmatrix} \begin{bmatrix} v_{xi}^{(n)} \\ v_{yi}^{(n)} \\ v_{xj}^{(n)} \\ v_{yj}^{(n)} \\ v_{xm}^{(n)} \\ v_{ym}^{(n)} \end{bmatrix} \right)$$

5. The third item

While for the third item, due to the boundary of material regiment (as in Fig. 1) is composed of the boundary of the Euler element grid (as in Fig. 3) plus the displacement field within the element.

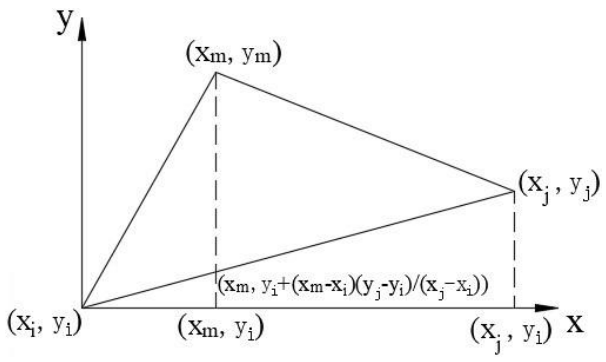

Fig. 3 the boundary of the Euler element grid

The lengths of the three edges of material regiment are as follows:

$$s_{ij} = \sqrt{(y_j + u_{yj} - y_i - u_{yi})^2 + (x_j + u_{xj} - x_i - u_{xi})^2},$$

$$s_{jm} = \sqrt{(y_m + u_{ym} - y_j - u_{yj})^2 + (x_m + u_{xm} - x_j - u_{xj})^2},$$

$$s_{mi} = \sqrt{(y_i + u_{yi} - y_m - u_{ym})^2 + (x_i + u_{xi} - x_m - u_{xm})^2}.$$

In order to facilitate the numerical calculation, the coordinate system is transformed into the natural coordinate system.

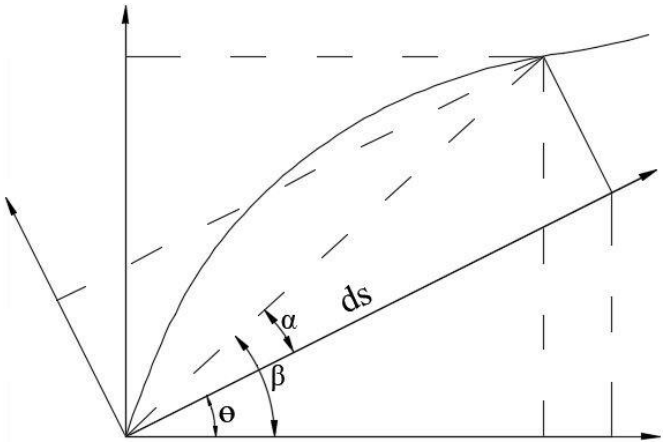

Fig. 4 The transformation of the coordinate between two different coordinate systems

As in Fig. 4, the transformation of the coordinate between the two different coordinate systems obeys

$$x = x_\tau \cos\theta - y_\tau \sin\theta, \quad y = x_\tau \sin\theta + y_\tau \cos\theta.$$

Where x_τ, y_τ are the variables in the natural coordinate system. The trigonometric functions corresponding to the three edges of material regiment are as follows:

$$\cos\theta_{ij}=\frac{x_j+u_{xj}-x_i-u_{xi}}{s_{ij}},\quad \sin\theta_{ij}=\frac{y_j+u_{yj}-y_i-u_{yi}}{s_{ij}},$$

$$\cos\theta_{jm}=\frac{x_m+u_{xm}-x_j-u_{xj}}{s_{jm}},\quad \sin\theta_{jm}=\frac{y_m+u_{ym}-y_j-u_{yj}}{s_{jm}},$$

$$\cos\theta_{mi}=\frac{x_i+u_{xi}-x_m-u_{xm}}{s_{mi}},\quad \sin\theta_{mi}=\frac{y_i+u_{yi}-y_m-u_{ym}}{s_{mi}}.$$

Then

$$\rho\oint_{\partial(\Omega-\Omega_e)} v(v\cdot \mathrm{n})\mathrm{d}s=\rho\oint_{\partial(\Omega-\Omega_e)}\begin{bmatrix} N_iN_i & 0 & N_iN_j & 0 & N_iN_m & 0\\ 0 & N_iN_i & 0 & N_iN_j & 0 & N_iN_m\\ N_iN_j & 0 & N_jN_j & 0 & N_jN_m & 0\\ 0 & N_iN_j & 0 & N_jN_j & 0 & N_jN_m\\ N_iN_m & 0 & N_jN_m & 0 & N_mN_m & 0\\ 0 & N_iN_m & 0 & N_jN_m & 0 & N_mN_m \end{bmatrix}$$

$$\begin{bmatrix} v_{xi}\\ v_{yi}\\ v_{xj}\\ v_{yj}\\ v_{xm}\\ v_{ym} \end{bmatrix}\left(\begin{bmatrix} N_i & 0 & N_j & 0 & N_m & 0\\ 0 & N_i & 0 & N_j & 0 & N_m \end{bmatrix}\begin{bmatrix} v_{xi}\\ v_{yi}\\ v_{xj}\\ v_{yj}\\ v_{xm}\\ v_{ym} \end{bmatrix}\cdot\begin{bmatrix} \sin\theta\\ -\cos\theta \end{bmatrix}\right)\mathrm{d}x_\tau$$

6. Verification and validation

In order to verify our proposed method, we did some test cases.

Firstly, just as in Fig. 5, we did a test case of the wave propagation in a rod. In this case, all the physical process of solid mechanics occurs in a fixed mesh without the mesh moving, by this way, we could compare the results of different numerical method with different variables. Just as in Fig. 6, we get the result that the results of the new method are the same as the results in the old method which calculates the solid mechanics with Lagrange variables, which means that the results of the new method calculating the solid mechanics with Euler variables obey the physical process of the solid mechanics.

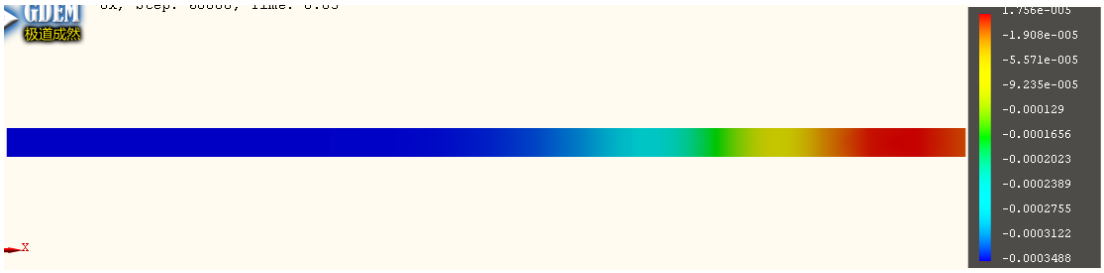

Fig. 5 Test case of wave propagation in a rod

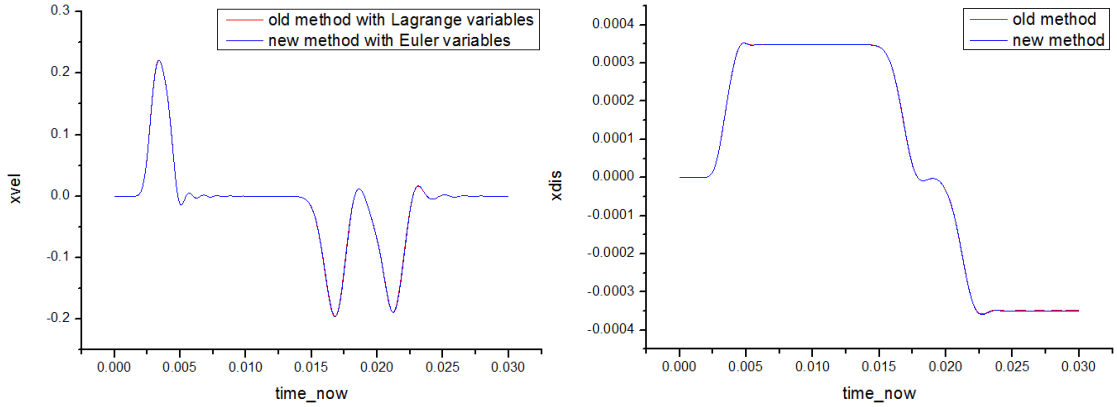

Fig. 6 Results of the first test case

Secondly, we did a test case of a slider sliding on a slope. The length of the slop is 1000 meters and the height of the slop is 200 meters. We let the friction coefficient of the slop equal to 0.3.

In this case, we use the fixed Euler grids to calculate, we use the boundary of material regiment to describe the movement of the boundary of slider, and after the boundary of material regiment moves beyond the Euler element grid size, new Euler element grid will appear and the corresponding old Euler element grid will disappear. By this way, the movement of slider could be calculated in the Euler fixed grids. The result is as in the figure 7 :

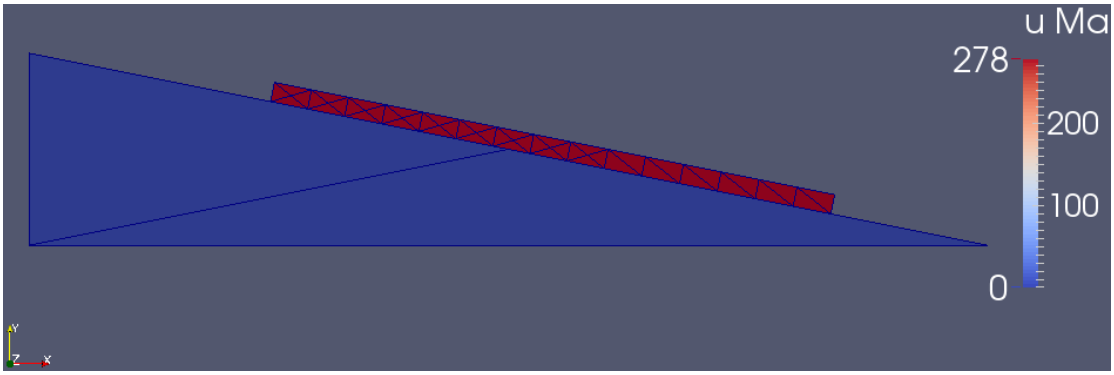

Fig. 7 Test case of slider sliding on a slope

The curves of the variation of velocity and displacement with time are as in the figure 8 :

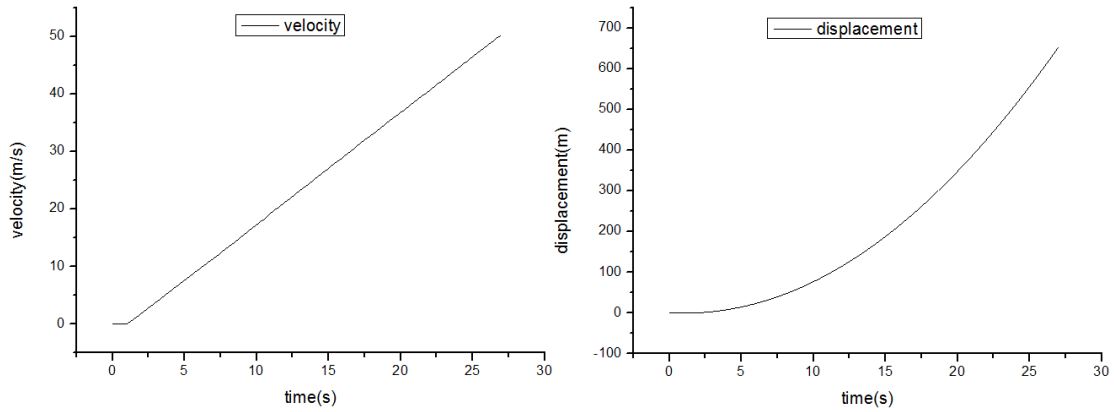

Fig. 8 Curves of the variation of velocity and displacement with time

From the figures, we could know that the variation of the velocity is the first order curve and the curve of the variation of displacement is quadratic curve, which obeys the moving law of the solid mechanics. And the acceleration gotten in the numerical results is 1.635, which equals to the corresponding mathematical results. Then we could get the result that the new method which calculates the solid mechanics with Euler variables is right and could be used to calculate the solid mechanic problems.

7. Conclusions

In this work, we proposed a numerical method for analyzing the solid mechanics with Euler variables. By replacing the Lagrange variables with the Euler variables, there will be three new items appearing in the equation. We use the fixed Euler grid to calculate solid mechanics, and use the boundary of material regiment to describe the movement of the boundary of material, after the boundary of material regiment moves beyond the Euler element grid size, new Euler element grid will appear and the corresponding old Euler element grid will disappear. By this way, the movement of solid could be calculated in the Euler fixed grids. Then we did some test cases, we get the result that the new method is right and could be used to calculate the solid mechanic problems.

Acknowledgement:

This work is supported by The National Natural Science Foundation of China (Grant No. 61807006) a nd The Natural Science Foundation of the Jiangsu Higher Education Institutions of China (No.18KJD1 10001).

References

[1] ZENG Tao, DENG Yunkai, HU Cheng, TIAN Weiming (2019) Development State and Application Examples of Ground-based Differential Interferometric Radar. Journal of Radars, 2019, Vol. 8, No. 1.
[2] GUO Zizheng, YIN Kunlong, HUANG Faming, LIANG Xin (2018) Landslide displacement prediction based on surface monitoring data and nonlinear time series combination model. Chinese Journal of Rock Mechanics and Engineering, 2018, Vol. 37, No. 1.
[3] GUO Sen, WANG Yujie (2018) Application of Ground-based Interferometric Synthetic Aperture Radar in Monitoring Deformation. GEOMATICS & SPATIAL INFORMATION TECHNOLOGY, 2018, Vol. 41, No. 12.
[4] Du Sunwen (2017) GB-SAR Open-pit Mine Slope Deformation Monitoring Data Analysis and

Prediction Method Research. Taiyuan University of Technology.
[5] Han Linfeng, Wang Pingyi (2018) Prediction of the maximum near-field wave amplitude of impulse waves generated by three-dimensional landslides based on momentum balance. Chinese Journal of Rock Mechanics and Engineering, 2018, Vol. 37, No. 11.
[6] C.A. Coulomb, An attempt to apply the rules of maxima and minima to several problems of stability related to architecture, Mem. Acad. R. Sci. 7 (1776) 343-382.
[7] J. Tinsley Oden, E.B. Pires, Nonlocal and nonlinear friction laws and variational principles for contact problems in elasticity, 1983.
[8] Tod A. Laursen, Formulation and treatment of frictional contact problems using finite elements, 1993.
[9] James Kenneth Mitchell, Kenichi Soga, et al., Fundamentals of Soil Behavior, Vol. 3, Jojn Wiley & Sons New York, 2005.
[10] L. De Lorenzis, I. Temizer, P. Wriggers, G. Zavarise, A large deformation frictional contact formulation using NURBS-based isogeometric analysis, Internat. J. Numer. Methods Engrg. 87 (13) (2011) 1278-1300.
[11] Chuanqi Liu, WaiChing Sun (2020) ILS-MPM: An implicit level-set-based material point method for frictional particulate contact mechanics of deformable particles, Computer Methods in Applied Mechanics Engineering 369 (2020) 113168.
[12] Peter A. Cundall, Formulation of a three-dimensional distinct element model-Part I. A scheme to detect and represent contacts in a system composed of many polyhedral blocks, Int. J. Rock Mech. Min. Sci. Geomech. Abstr. 25 (3) (1988) 107-116.
[13] Kun Wang, WaiChing Sun, A semi-implicit discrete-continuum coupling method for porous media based on the effective stress principle at finite strain, Comput. Methods Appl. Mech. Engrg. 304 (2016) 546-583.
[14] Yang Liu, WaiChing Sun, Jacob Fish, Determining material parameters for critical state plasticity models based on multilevel extended digital database, J. Appl. Mech. 83 (1) (2016) 011003.
[15] G.T. Houlsby, Potential particles: a method for modelling non-circular particles in DEM, Comput. Geotech. 36 (6) (2009) 953-959.
[16] Jose E. Andrade, Keng-Wit Lim, Carlos F. Avila, Ivan Vlahinic, Granular element method for computational particle mechanics, Comput. Methods Appl. Mech. Engrg. 241 (2012) 262-274.
[17] Peter Wriggers, Giorgio Zavarise, Computational contact mechanics, Encyclopedia Comput. Mech. (2004).
[18] Giorgio Zavarise, Laura De Lorenzis, The node-to-segment algorithm for 2D frictionless contact: classical formulation and special cases, Comput. Methods Appl. Mech. Engrg. 198 (41-44) (2009) 3428-3451.
[19] Michael A. Puso, Tod A. Laursen, A mortar segment-to-segment contact method for large deformation solid mechanics, Comput. Methods Appl. Mech. Engrg. 193 (6-8) (2004) 601-629.
[20] M. Tur, F.J. Fuenmayor, P. Wriggers, A mortar-based frictional contact formulation for large deformations using Lagrange multipliers, Comput. Methods Appl. Mech. Engrg. 198 (37-40) (2009) 2860-2873.
[21] Brandon K. Zimmerman, Gerard A. Ateshian, A surface-to-surface finite element algorithm for large deformation frictional contact in FEBio, J. Biomech. Eng. 140 (8) (2018) 081013.
[22] Takashi Nomura (1994) ALE finite element computations of fluid-structure interaction problems. Computer Methods in Applied Mechanics and Engineering 112 (1994) 291-308.
[23] Yue Bao-zeng (2006) ALE Fractional Step Finite Element Method for Fluid-Structure Nonlinear Interaction Problem. Journal of Beijing Institute of Technology, 2006, Vol. 15, No. 1.
[24] Rohan Abeyaratne (2012) Continuum Mechanics. Volume II of Lecture Notes on The Mechanics of Elastic Solids. MIT Department of Mechanical Engineering.
[25] KEITH CONRAD. Differentiating Under the Integral Sign.
[26] Harley Flanders (1973) Differentiation Under the Integral Sign. The American Mathematical Monthly, Vol. 80, No. 6 (Jun. - Jul., 1973), pp. 615-627.
[27] Liu Haihu, Li Kaitai, Su Jian, Wang Shangjin (2006) Operator Splitting Methods for Solution of Incompressible Viscous Flows. Journal of Xi'an Jiaotong University, 2006, Vol. 40, No. 12.

[28] Shui Qing-xiang, Wang Da-guo (2014) Numerical solution for unsteady incompressible N-S equations by least-squares-based operator-splitting finite element method. Chinese Journal of Computational Mechanics, 2014, Vol. 31, No. 5.
[29] Sun Xu, Zhang Jiazhong (2011) A Characteristic-Based Split-FEM Scheme for Incompressible Viscous Flow with Moving Boundaries. Journal of Xi'an Jiaotong University, 2011, Vol. 45, No. 1.
[30] Tao Yongfa, Yang Yisheng, Wang Chengquan (1994) The Problem of Plastic Plane Compression Solved by the Energy Method in Comoving Curvilinear Coordinate. Journal of Northeast Heavy Machinery Institute, 1994, Vol. 18, No. 3.